International Journal of Mass Spectrometry xxx (xxxx) 116860

Contents lists available at ScienceDirect

International Journal of Mass Spectrometry

journal homepage: www.elsevier.com/locate/ijms

Calculated rate coefficients between CI-MS reagent ions and organosulfur compounds causing food taints and off-flavours

Manjeet Bhatia [a, b, *], Nicola Manini [a], Franco Biasioli [b], Luca Cappellin [b, c]

[a] Dipartimento di Fisica, Università Degli Studi di Milano, Via Celoria, 16, I, 20133, Milano, Italy
[b] Department of Food Quality and Nutrition, Research and Innovation Centre, Fondazione Edmund Mach, 38010, San Michele All'Adige, TN, Italy
[c] Dipartimento di Scienze Chimiche, Università Degli Studi di Padova, Via Marzolo 1, 35121, Padua, Italy

ARTICLE INFO

Article history:
Received 28 February 2022
Received in revised form 21 April 2022
Accepted 24 April 2022

ABSTRACT

Volatile sulfur compounds play a crucial role in the aroma profile of food and fermented beverages. We explore chemical-ionization mass spectrometry (CI-MS) ion-molecule reaction kinetics of commonly used reagent ions to a list of volatile organic sulfur compounds (VOSCs). We compute the rate coefficients of ion-molecule reactions, useful for the accurate identification and quantification of trace gases, using capture collision models based on the electric dipole moment and polarizability of the neutral VOSCs. To this aim, we evaluate molecular properties, such as the electric dipole moment, polarizability, proton affinity (PA), and ionization energy (IE) for each VOSC, by means of hybrid density functional theory (DFT) simulations. The PA and IE values are useful in the selection of appropriate reagent ions to be used in CI-MS. We thoroughly investigate collision rate coefficients at effective temperatures and internal energies, as relevant for highly energetic proton transfer reaction mass spectrometry (PTR-MS) drift tube conditions. The data provided will be valuable for the rapid quantification of VOSCs in food and fermented beverages.

1. Introduction

Volatile organic sulfur compounds (VOSCs) critical to aroma in food and beverages, especially those with reduced form of sulfur, are attributed to microbiological degradation, processing, packaging, and storage conditions of ingredients and finished products [1–4]. An excessive concentration of compounds containing sulfur, which originate from natural sources, typically contributes to off-flavor in many food products, particularly those involving fermentation, and leads to consumer dislike and eventually to the rejection of the products. Sulfur being a larger and active hetero atom with smaller electronegativity than oxygen, its presence greatly influences the relative reactivity of the compounds carrying sulfur, compared to their oxygen equivalent. A range of VOSCs can be present in food and beverages, with some contributing positive 'fruity' character at low concentration, and others imparting unwanted 'reductive' aromas similar to "rotten eggs", "natural gas", and "onion" at high concentration. VOSCs contribute to food aroma and flavor in a complex way, as their sensory thresholds are typically low, often a few parts per trillion by volume (pptv). The low concentration of flavor compounds in food and beverages has made their isolation, separation, and analysis problematic. Commonly present sulfur compounds, with their characteristic flavor and threshold, include hydrogen sulfide (rotten egg [1000 ng/L]), methanethiol (putrefaction, onion, rubber [2000 ng/L]), dimethylsulfide (cabbage, asparagus [25000 ng/L]); polyfunctional thiols, such as 4-mercapto-4-methylpentan-2-one (box tree, guava [3 ng/L]); S-heterocycle compounds like benzothiazole (rubber [50 ng/L]), and aryl thiols, such as 2-furanmethanethiol (roasted coffee [0.4 ng/L]) [5,6].

The chemical complexity and low concentration of VOSCs in foods put an analytic challenge in their detection and quantification. Due to the high activity of VOSCs, rapid and accurate analytic methods are required in order to minimize artifacts during sample handling, storage, and pre-treatment prior to analysis. Direct-injection mass spectrometry (DIMS) techniques, such as proton-transfer reaction mass spectrometry (PTR-MS) [7] and selected ion flow mass spectrometry (SIFT-MS) [8] have been powerful tools in VOSCs identification and quantification, especially for flavor analysis. In particular, PTR-MS is mostly used in sensory predictions and aroma release or quality control in food science, specifically in the analysis of fermented food products. PTR-MS is an ideal technique for VOSCs analysis since it eliminates time-consuming and artifact-prone sample preparation. Moreover, PTR-MS provides fast analysis time, high detection sensitivity, and real-time

* Corresponding author. Dipartimento di Fisica, Università degli Studi di Milano, Via Celoria, 16, I, 20133, Milano, Italy.
E-mail address: manjeetbhatia83@gmail.com (M. Bhatia).

https://doi.org/10.1016/j.ijms.2022.116860
1387-3806/© 20XX

analysis of trace-level compounds, thus a preferred technique in environmental, food science, medical, and biological science [9–12].

PTR-MS has been extensively used for the characterization of VOSCs in various fields including food aroma analysis. Schuhfried et al. studied chemical ionization based fragmentation of sulfides using PTR-MS [13]. VOSCs have been analyzed in Swiss cheese using PTR-MS by Harper and co-workers [14]. Other similar studies devoted to sulfur compounds adopted the PTR-MS technique [11,15]. In parallel, the theoretical computation of rate coefficients has also been carried out, e.g. by Cappellin et al. [16]. In the PTR-MS instrument, the H_3O^+ ions ionize the sample gas through a proton transfer reaction occurring in a drift tube chamber. The electric field is applied in the drift tube chamber, which escalates the ion kinetic energy, and as a result, water cluster formation is greatly reduced. The sample gas with higher proton affinity (PA) than H_2O readily acquires a proton from H_3O^+ ion via exothermic proton-transfer reaction. The resulting protonated VOC.H^+ ions are detected by a mass analyzer, see Fig. 1. Then the concentration of a neutral volatile organic compound (VOC) is determined by calibrating the instrument with a standard of known concentration and protonated ion signals. For the most accurate results, the PTR-MS instrument should be calibrated for every single VOC in a complex gas mixture. However, this procedure is laborious, time-consuming, and in practice, it is not possible to have accurate standards for every VOCs detected by PTR-MS. Alternatively, the PTR-MS concentration of VOCs can be determined by measuring the protonated VOC.H^+ and reagent ion H_3O^+ counts. Given the rate coefficient of the proton-transfer reaction, which depends on the reaction kinetics occurring in the drift tube [17], concentrations can be estimated.

Su and co-workers provided several theoretical or numerical approaches aiming at ion-molecule collision reactions taking place in drift tube chamber. These approaches include the average dipole orientation (ADO) [18,19], classical trajectory calculations [20], and the parametrized classical trajectory method [21] to evaluate collision rate coefficients, k_c. These methods take the molecular polarizability and the electric dipole moment of the VOCs as input parameters. In particular, the parameterized trajectory model estimates collision rate coefficients as a function of the center-of-mass energy and temperature under PTR-MS drift tube conditions. Strongly exothermic ion-molecule reactions are expected to proceed at collision rates, therefore the reaction rate coefficients (k) are given by the collision rates (k_c). Previous studies of H_3O^+, NO^+ and O_2^+ reactions with several organosulfur molecules have established that most of the reactions occur at or close to their collision rates

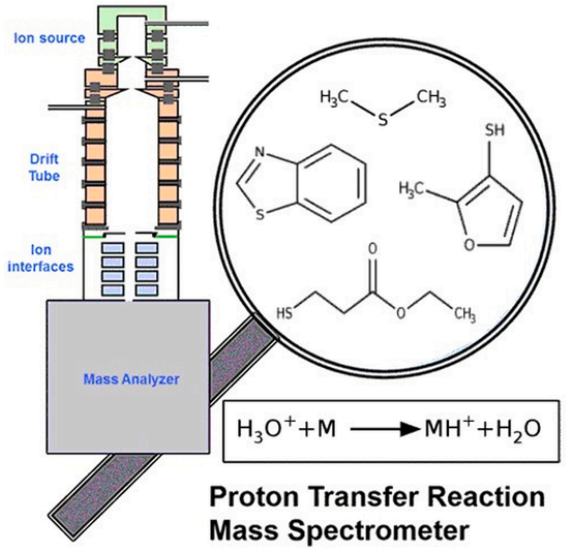

Fig. 1. A basic schematic of PTR-MS instrument, where H_3O^+ ion, commonly used reagent ion, transfers proton to neutral molecule M.

$k \simeq k_c$ [22,23]. However, there are molecules for which the reactions with some primary ions do not proceed at collision rates [24].

2. Overview

2.1. PTR/CI-MS mass spectrometry

Conventional PTR-MS instrument uses H_3O^+ reagent ion as a primary proton donor to ionize many types of volatile compounds. However, modern chemical ionization mass spectrometry (CI-MS) instruments allow the operator to switch between different reagent ions [25–27], being capable of exploiting reagent ions other than H_3O^+, simply by passing a different reagent gas through the ion source. Frequently used ions in such CI-MS include NH_4^+, NO^+, and O_2^+, which have been applied efficiently for the ionization of the VOSCs [6,14,22]. These chemical-ionization methods are more or less selective to a certain class of VOCs or have functional-group-dependent ionization mechanisms. As a result, the functional group of a specific detected VOC.H^+ ion can be determined. Molecules such as ethylene, acetylene, halocarbons and common small-molecular weight gases, such as SO_2 cannot be ionized by the H_3O^+ ion. However, all of these substances can be detected and quantified with CI-MS instrument by adopting an appropriate reagent ion through fast switching among several reagent ions, in usually less than 10 s. The adoption of NH_4^+, NO^+, and O_2^+ reagent ions results in procuring VOC sensitivities in the same order as with the H_3O^+ ion. Other advantages of CI-MS include isobaric separation and a higher level of selectivity in VOC identification and quantification.

2.2. Proton-transfer reactions in CI/PTR-MS

The measurement of ion signals, preferably the ion signal ratio (proton acceptor/proton donor) by mass spectrometer, allows scientists to measure the absolute concentration of a specific constituent of a gas mixture. In PTR-MS, the reaction between H_3O^+ and an analyte sampled species M,

$$H_3O^+ + M \longrightarrow MH^+ + H_2O, \quad (1)$$

represents proton transfer from the hydronium ion to the analyte M, by a first-order pseudo reaction. Such a reaction is effective when the PA of the acceptor molecule, M, exceeds that of the H_2O molecule (166.7 kcal/mol), which makes the proton transfer thermodynamically feasible. The absolute concentration [M] of the analyte in reaction [1] can be determined by measuring the respective ion signals of protonated analyte, M, and the reagent ion H_3O^+ as in equation [2] below,

$$\frac{[RH^+]}{[H_3O^+]} = \frac{i(RH^+)}{i(H_3O^+)} = k[M]t, \quad (2)$$

and finally,

$$[M] = \frac{1}{k\,t}\frac{[RH^+]}{[H_3O^+]}. \quad (3)$$

Here k is the reaction-rate coefficient and t represents the reaction time, usually $\sim 100\ \mu s$ in a typical PTR-MS instrument. The concentration [M] in principle can be determined without calibration simply by recording the ratio of the MH^+ ion counts to those of the H_3O^+, provided reaction rate coefficient k is known already. It is worthwhile to mention that dissociation and fragmentation may occur upon reaction between compounds, especially alcohols and H_3O^+. Thereby, the product ion counts could differ from as assumed in the above equations.

Su, Bowers and Chesnavich provided many theoretical methods for estimating rate coefficients of exothermic ion-molecule reactions of type [1]. The most successful method which predicts the rate coefficients consistent with (mostly room-temperature) experiments is the average dipole orientation (ADO) [18,19]. At elevated internal energies

the classical trajectory method, dependent on center-of-mass energy given by Su and co-workers [21] is to be preferred. Usually, room-temperature rate coefficients are employed for quantitative analysis in PTR-MS. This is however not strictly true, since ion-molecule collisions inside the drift tube are often far more energetic than at room-temperature ion-molecule collisions. Due to the applied electric field, the translational energy of the colliding ions leads to the center-of-mass energy largely exceeding the energy typical of thermal collisions. A quantitative description of total mean ion kinetic energy of the ions in the drift tube is given by Wannier [28,29] and McFarland [30]. They showed that the total kinetic energy of an ion can be written as

$$KE_{\text{ion}} = \frac{3}{2}k_{\text{B}}T + \frac{1}{2}m_{\text{ion}}v_d^2 + \frac{1}{2}m_b v_d^2, \tag{4}$$

where m_{ion} is mass of the ion, v_d is drift velocity of the ion, and m_b is mass of the buffer gas. k_{B} is the Boltzmann's constant. The center-of-mass kinetic energy for an ion-neutral molecule collision is then obtained by the following expression:

$$KE_{\text{com}} = \frac{3}{2}k_{\text{B}}T + \left(\frac{m_n}{m_{\text{ion}} + m_n}\right)\left(KE_{\text{ion}} - \frac{3}{2}k_{\text{B}}T\right), \tag{5}$$

In the above equation, m_{n} represents the mass of the neutral molecule. These highly energetic conditions inside the drift tube give rise to a higher effective temperature, T_{eff}, for ion-molecule collisions in PTR-MS. T_{eff} can be obtained by equating an effective ion thermal energy with the mean center-of-mass collision energy between the ion and the buffer gas [17]. The expression for the effective temperature T_{eff} results in

$$T_{\text{eff}} = T + \left(\frac{v_d^2}{3k_{\text{B}}}\right)\left[\frac{m_n\left(m_{\text{ion}} + m_b\right)}{m_{\text{ion}} + m_n}\right]. \tag{6}$$

Here T is the drift-tube temperature, and the remaining terms are as defined earlier. For normal PTR-MS conditions, i.e. v_d = 906 m s^{-1}, E/N =120 Td (where E/N is the ratio of electric field to gas number density and Td = Townsend = 10^{-21} V m^2) and T = 300 and 380 K, the predicted value of T_{eff} for H_3O^+ reagent ion is typically much higher than 1000 K. The T_{eff} for the hydrogen sulfide at T = 300 and 380 K is found to be 1316 and 1396 K, respectively. These figures indicate that room-temperature rates are not suitable for the highly energetic ion-molecule collisions inside the PTR-MS drift tube.

2.3. Switchable reagent ions in CI-MS

The key advantages of using H_3O^+ as a proton donor are: (i) It does not react with main air constituents, as their PA value is lower than the H_2O molecule; (ii) most common VOCs have higher PAs than H_2O such that proton transfer occurs exothermally on every collision. However, dealing with the analytes that possess higher PA than H_2O and separating isomers are major concerns with H_3O^+ reagent ions. These issues pave the way for other reagent ions to be used in CI-MS. Reagent ions, such as NH_4^+, NO^+, and O_2^+ have been applied efficiently for the ionization of the VOSCs, Fig. 2 [6,14,22].

Ionization via NH_4^+ ions, typically called NH_4^+-CI-MS, offers high VOC selectivity due to the higher PA of NH_3 (204.0 kcal/mol) compared to H_3O^+ ion. This higher selectivity has been recognized as an efficient way in the identification of isobaric compounds. NO^+ ions ionize the VOCs by electron transfer when the ionization energy (IE) of the analyte is less than that of NO molecule, i.e. 9.3 eV. The NO^+ reagent ion, upon reacting with an analyte molecule, can be helpful to support isomeric compounds separation in CI-MS analysis [31,32]. For primary ions such as NH_4^+ and NO^+ reactions other than charge transfer and proton transfer are possible for VOCs [33–35]. For instance, cluster ion chemistry in NH_4^+-CI-MS may take place. In order to get insights into this reaction channel, PA alone may not be sufficient, bond energies (BE, in enthalpy) of cluster ions and reaction enthalpies ΔH_r of reaction ($NH_4^+A \rightarrow AH^+ + NH_3$) should be used instead [33]. Furthermore, study of hydride abstraction and cluster formation may provide even more insights into NO^+-CI-MS reactions other than electron transfer. Future work could be undertaken to investigate reaction modes of VOSCs in CI-MS other than proton transfer and electron transfer.

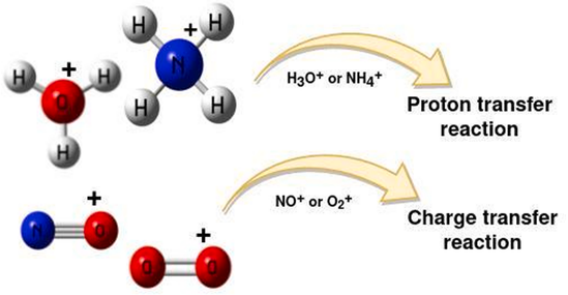

Fig. 2. Common reactions of primary reagent ions with VOSCs. However, it is worthwhile to note that other modes of reactions are possible with the selected reagent ions based on the PA and IE difference between reagent ion and neutral molecule.

Similarly, the O_2^+ reagent ion reacts through electron transfer if the analyte molecule possesses lower IE than the O_2 molecule (12.1 eV) thus ionizing molecules that cannot be ionized by the H_3O^+ and NO^+ ions. Due to the large available energy compatible with the IE of the analyte and the electron affinity of the selected reagent ion, the molecule may fragment into many products.

3. Computational method

To evaluate the following molecular properties: electric dipole moment, polarizability, PA, and IE of several VOSCs, we perform electronic-structure simulations using the Gaussian16 software suite [36]. We opt for the B_3LYP [37] exchange and correlation functional, a standard approach for gas-phase systems. We expand the Kohn-Sham wave functions on an Aug-cc-PVTZ basis set for the evaluation of molecular properties of VOSCs. Presently, the Aug-cc-PVTZ is regarded as an optimal basis set for high-accuracy computations, with the only disadvantage of being computationally rather expensive. The Aug-cc-PVTZ basis set has the advantage of being correlation consistent, i.e. this basis set is optimized using correlated methods. Overall, the adopted DFT method provides a good combination of cost vs accuracy.

We retrieved all initial molecular structures from standard databases, such as NIST [38] and PubChem [39]. Starting from these structures, we perform structural optimizations, minimizing the total DFT energy. In the resulting optimized geometry of the neutral VOSCs, we evaluate the electric dipole moment, polarizability, PA, and IE values. As we target ambient conditions inside SRI/PTR-MS drift tube, gas-phase properties are considered, and no environmental effects, such as, e.g., due to a solution, are included. Based on the obtained electric-dipole moment and polarizability, we compute the rate coefficients of ion-molecule reactions using capture collision models.

4. Results and discussion

Table 1 reports the computed molecular properties. The listed electric dipole moment and polarizability values are in close agreement with literature values, where available. Tables 2 and 3 compares our simulated results with the few available experimental and numerical results. The proton transfer from H_3O^+ or NH_4^+ ions in PTR-MS drift tube is exothermic when the PA of the analyte molecule exceeds the PA of H_2O or NH_3 molecules, respectively. All the molecules under exploration possess higher PAs than H_2O, thus indicating their propensity towards exothermic proton-transfer reactions. Hydrogen sulfide has a PA only slightly higher than water; when H_3O^+ is used as primary ion, there is a strong humidity dependence of the PTR-MS measurements [40]. When proton transfer is relatively exothermic by more than approximately 23 kcal/mol, then dissociative proton transfer is likely to occur from $[MH^+]^*$ and leads to fragmentation and more complicated mass spectra [41]. When investigating certain VOSCs such as, e.g, diethyl sulfide, 4-mercapto-4-methylpentan-2-ol, benzothiazole, 2-

Table 1
Computed molecular data, namely: electric dipole moment; dielectric polarizability; proton affinity (PA); and ionization energy (IE), for sulfur compounds of which traces may contaminate food and beverages. DFT results obtained with a B_3LYP functional and Aug-cc-PVTZ basis, using the Gaussian suite [36].

Molecule name (Formula)	CAS Number	Dipole Moment	Polarizability	PA	IE
Molar mass (atomic units)		μ_D (Debye)	$\alpha/(4\pi\varepsilon_0)$ (Å^3)	kcal/mol	eV
Hydrogen Sulfide (H_2S) 34.08	7783-06-4	0.99	3.71	169.1	10.4
Methanethiol (CH_4S) 48.11	74-93-1	1.56	5.55	186.1	9.4
Ethanethiol (C_2H_6S) 62.14	75-08-1	1.68	7.43	190.6	9.2
Dimethyl Sulfide (C_2H_6S) 62.14	75-18-3	1.60	7.46	199.3	8.6
Diethyl Sulfide ($C_4H_{10}S$) 90.19	352-93-2	1.64	11.34	206.3	8.3
Dimethyl Disulfide ($C_2H_6S_2$) 94.20	624-92-0	2.03	10.79	193.7	8.1
Diethyl Disulfide ($C_4H_{10}S_2$) 122.3	110-81-6	2.15	14.67	197.8	7.9
Methyl Thioacetate (C_3H_6OS) 90.15	1534-08-3	1.36	9.64	198.5	9.1
3-Mercaptohexan-1-ol ($C_6H_{14}OS$) 134.24	51755-83-0	1.68	15.43	196.6	8.6
4-Mercapto-4-methylpentan-2-one ($C_6H_{12}OS$) 132.23	19872-72-7	2.27	14.86	198.2	8.5
4-Mercapto-4-methylpentan-2-ol ($C_6H_{14}OS$) 134.24	255391-65-2	2.53	15.34	204.7	8.5
Benzothiazole (C_7H_5NS) 135.19	95-16-9	1.34	15.91	220.7	8.6
2-Furanmethanethiol (C_5H_6OS) 114.17	98-02-2	1.94	12.81	199.1	8.1
2-Mercaptoethanol (C_2H_6OS) 78.14	60-24-2	2.50	8.14	193.4	9.0
Benzenemethanethiol (C_7H_8S) 124.21	100-53-8	1.48	15.74	195.3	8.3
2-Mercaptoethyl acetate ($C_4H_8O_2S$) 120.17	5862-40-8	1.83	11.91	199.2	9.1
3-mercaptopropyl acetate ($C_5H_{10}O_2S$) 134.20	26473-61-0	1.61	13.97	199.6	9.0
Cis-3,6-dimethyl-1,2,4,5-tetrathiane ($C_4H_8S_4$) 184.40	75100-46-8	0	19.83	196.1	8.0
Prenyl-mercaptan ($C_5H_{10}S$) 102.20	5287-45-6	1.78	13.35	198.2	8.1
Trans-3,6-dimethyl-1,2,4,5-tetrathiane ($C_4H_8S_4$)	75100-47-9	0	19.11	195.3	8.3

Table 1 (*continued*)

Molecule name (Formula)	CAS Number	Dipole Moment	Polarizability	PA	IE
184.80					
2-Methyl-3-furanthiol (C_5H_6OS) 114.17	28588-74-1	0.90	12.47	190.3	7.7
2-Methylthiolane-3-ol ($C_5H_{10}OS$) 118.20	149834-43-5	2.12	12.71	207.5	8.2
3-Mercapto-3-methylbutan-1-ol ($C_5H_{12}OS$) 120.22	34300-94-2	1.84	13.52	197.7	8.6
Ethyl-3-mercaptopropionate ($C_5H_{10}O_2S$) 134.20	5466-06-08	2.76	13.91	196.7	8.9
5-2-hydroxyethyl-4-methylthiazole (C_6H_9NOS) 143.21	137-00-8	2.79	15.29	229.7	8.1
2-Methyltetrahydro thiophen-3-one (C_5H_8OS) 116.18	13679-85-1	1.72	12.14	196.1	8.6
3-Methylsulfanyl propan-1-ol ($C_4H_{10}OS$) 106.19	0505-10-02	3.06	12.03	203.1	8.4
3-Mercaptohexylacatate ($C_8H_{16}O_2S$) 176.28	136954-20-6	1.47	19.32	194.9	8.8
Ethylthioacetate (C_4H_8OS) 104.17	625-60-5	1.41	11.57	201.2	9.0

Table 2
Comparison of the computed electric dipole moment and polarizability values of volatile sulfur compounds using B_3LYP DFT functional and Aug-cc-PVTZ basis set combination with the available experimental/theoretical results.

Molecule	μ_D		$\alpha/(4\pi\varepsilon_0)$	
	(Debye)		(Å^3)	
	This work	Literature	This work	Literature
Hydrogen Sulfide (H_2S)	0.99	0.98 [46] 0.97 [47]	3.71	–
Methanethiol (CH_4S)	1.56	1.52 [46]	5.55	–
Ethanethiol (C_2H_6S)	1.68	1.61 [46]	7.43	7.41 [46]
Dimethyl Sulfide (C_2H_6S)	1.60	1.55 [46] 1.72 [48]	7.46	6.80 [48]
Diethyl Sulfide ($C_4H_{10}S$)	1.64	1.65 [46]	11.34	–
Dimethyl Disulfide ($C_2H_6S_2$)	2.03	1.85 [46]	10.79	–

methylthiolane-3-ol, and 5-2-hydroxyethyl-4-methylthiazole characterized by much higher PAs than the water molecule, it is worthwhile to analyze these compounds with NH_4^+ ions, thereby obtaining cleaner spectra. However, CI-MS-NH_4^+ reactions can proceed by association when the PA of the analyte is close to that of NH_3.

Similarly, electron transfer in CI-MS from NO^+ or O_2^+ reagent ions occurs exothermally when the IE of the analytic compound is lower than the IE of the NO or O_2 molecule. From the IE data reported in Table 1, it is expected that NO^+ ion will efficiently transfer electron to all the VOSCs with exothermal reactions at every collision, except for the molecules that possess higher IEs than NO, for example hydrogen sulfide and methanethiol. In such cases, however, other reaction path-

Table 3
Comparison of the computed proton affinity (PA) and ionization energy (IE) values with the available experimental/theoretical results.

Molecule	PA		IE	
	(kcal/mol)		(eV)	
	This work	Literature	This work	Literature
Hydrogen Sulfide (H_2S)	169.1	–	10.4	–
Methanethiol (CH_4S)	186.1	184.9 [46]	9.4	–
Ethanethiol (C_2H_6S)	190.6	188.7 [46]	9.2	9.3 [46]
Dimethyl Sulfide (C_2H_6S)	199.3	198.6 [46] 198.6 [48]	8.6	8.7 [46]
Diethyl Sulfide ($C_4H_{10}S$)	206.3	204.7 [46]	8.3	8.4 [46]
Dimethyl Disulfide ($C_2H_6S_2$)	193.7	–	8.1	7.4 [46]
Diethyl Disulfide ($C_4H_{10}S_2$)	197.8	–	7.9	8.3 [46]

ways such as hydride abstraction may occur. For these large-IE compounds, O_2^+ ions can be used instead.

The molecular data reported in Table 1 are essential for the calculation of the rate coefficients for ion-molecule collision reactions that commonly occur in PTR/CI-MS drift tubes. Collision-based models are often used for the determination of rate coefficients, since a direct experimental determination of rate coefficients is often laborious, time-consuming, and even problematic, leading to errors up to ± 30% [42–44]. In the ion-nonpolar molecule, long-range ion–induced-dipole interactions dominate. The long-range potential in the ion–induced-dipole is given by

$$V(r) = -\frac{1}{4\pi\varepsilon_0}\frac{\alpha q^2}{2r^4}, \tag{7}$$

where $q = z\,q_e$ is the charge of the ion (q_e is the elementary charge in Coulomb); α is the polarizability of the neutral species, r is the distance between the centers of mass of the ion and neutral molecule. The rate coefficient (capture) is given by the Langevin theory, and the expression reads as

$$k_{lang} = \sqrt{\frac{\pi\alpha q^2}{\mu\varepsilon_0}}. \tag{8}$$

Here μ is the reduced mass of the reactants, and ε_0 is the permittivity of free space. The rates obtained from the Langevin model, equation [8], seriously underestimate the observed rate coefficients, and are not suitable for reactions involving polar molecules. For polar molecules, a more refined model includes ion-dipole forces in addition to the ion–induced-dipole forces. In this case, the interaction potential takes the form

$$V(r,\theta) = -\frac{1}{4\pi\varepsilon_0}\frac{\alpha q^2}{2r^4} - \frac{1}{4\pi\varepsilon_0}\frac{q\mu_D}{2r^2}\cos\,\theta. \tag{9}$$

Here μ_D is the dipole moment of the neutral molecule and θ is the angle the dipole makes with the line of centers of the collision. The long range forces, ion-induced dipole and ion-permanent dipole forces contribute toward increasing rate coefficients. However, the extent of their contribution largely depends on the electric dipole moment.

Considering the energetic environment inside CI-MS drift tube, rates obtained at thermal conditions cannot be applicable as such in practical applications. Under the PTR/CI-MS highly energetic conditions, the rate coefficients can be obtained by parameterized trajectory calculations as given by Su [21] appropriate at center-of-mass kinetic energy and higher effective temperature. The parametrized rates are expressed by the following equations

$$\frac{k_{cap}}{k_{Lang}} = K_c(\tau,\varepsilon), \tag{10}$$

where

$$\tau = \frac{\mu_D}{\sqrt{\alpha T}}, \tag{11}$$

and

$$\varepsilon = \frac{\mu_D}{\sqrt{\alpha K E_{com}}}. \tag{12}$$

Su and co-workers simulated over 100 systems, processing 6000 trajectories. The following parametric equation was proposed to fit the simulation data:

$$K_c(\tau,\varepsilon) = 1 + c_1\tau^{0.4}\varepsilon^2 S + c_2(1-S) \times \sin\left[c_3\{c_4 + \ln(\tau)\}\right]\tau^{0.6}\sqrt{(\varepsilon - 0.5)}, \tag{13}$$

where $c_1 = 0.727143$, $c_2 = 3.71823$, $c_3 = 0.586920$ and $c_4 = 4.97894$. The quantity

$$S = \begin{cases} \exp[-2(\varepsilon - 1.5)] & \text{for } \varepsilon > 1.5 \\ 1 & \text{for } \varepsilon \le 1.5 \end{cases}. \tag{14}$$

The results obtained from the parametrized trajectory model are collected in Table 4. The rate coefficients k_{cap} dependent on center-of-mass energy are computed at standard PTR-MS working temperatures: 300 and 380 K, and reduced electric field E/N = 120 Td, under air as a buffer gas. However, the E/N values may vary from 80 to 155 Td for typical PTR-MS instruments.

The obtained rate coefficients decrease marginally with temperature, adherent to the theory, as well as observed in a few available experiments [45]. k_{cap} is also found to vary with the applied electric field or reduced electric field, which, in turn, increases the center-of-mass kinetic energy in the collision between the ion and the molecule. The variation of the reagent-ion temperature and ion translational energy (through E/N) provides a degree of control of the overall center-of-mass collision energy. The computed rate coefficients decrease with the center-of-mass kinetic energy due to the faster collision.

Importantly, the computed rates, as in Table 4 increase significantly with both the permanent dipole moment and the polarizability of the neutral species. VOSCs, such as 3-methylsulfanylpropan-1-ol and 5-2-hydroxyethyl-4-methylthiazole, possess relatively large dipole moments (greater than 2.5 Debye) resulting in rather large rate coefficients. In contrast, the smaller dipole moments (<1 Debye) of hydrogen sulfide and 2-methyl-3-furanthiol lead to smaller rate coefficients for these molecules. *Cis*-3,6-dimethyl-1,2,4,5-tetrathiane and *trans*-3,6-dimethyl-1,2,4,5-tetrathiane have exactly vanishing dipole moments. The rate coefficient for these species is essentially given by the Langevin rates due to the lack of an ion-dipole interaction ($\propto \mu_D$) contribution, as in equation [7] rather than [9].

When compared with experimental observations, the results of the rate coefficients from equation [13] were in good agreement (5% error) for ion-molecule collisions with center-of-mass energies ranging from thermal to several eV and over a temperature range 50–1000 K [21]. This reassures us that the rate coefficients obtained by means of the parameterized-trajectory method are reliable even at elevated temperature and internal-energy conditions.

Additionally, we compute the effective temperature, T_{eff}, from equation [6] under the standard working temperatures 300 and 380 K, considered in the present work. Also, collision rates at different E/N values in the 80–180 Td range are obtained for the reported reagent ions. The results are collected as supplementary material. At higher T_{eff}, the rates vary marginally, and in many cases, we obtain practically the same rate coefficients at two different temperatures. Thus, even in the case of a significant uncertainty about the actual temperature of the colliding species, the final reaction rates

Table 4
Predicted rate coefficients (k_{cap}) at center-of-mass energy under ambient PTR/SRI-MS drift tube settings from parametrized classical trajectory method for sulfur compounds commonly present in food and beverages. Computed rates are expressed in unit of 10^{-9} cm^3 s^{-1}.

Molecule name	*T*	k_{cap}			
(Formula)	K	H_3O^+	NH_4^+	NO^+	O_2^+
Hydrogen Sulfide	300	1.65	1.67	1.43	1.41
(H_2S)	380	1.61	1.64	1.39	1.38
Methanethiol	300	2.18	2.23	1.85	1.80
(CH_4S)	380	2.12	2.16	1.80	1.75
Ethanethiol	300	2.29	2.34	1.90	1.86
(C_2H_6S)	380	2.23	2.28	1.86	1.81
Dimethyl Sulfide	300	2.22	2.26	1.86	1.82
(C_2H_6S)	380	2.17	2.21	1.82	1.78
Diethyl Sulfide	300	2.37	2.44	1.95	1.91
($C_4H_{10}S$)	380	2.34	2.40	1.92	1.88
Dimethyl Disulfide	300	2.61	2.67	2.12	2.06
($C_2H_6S_2$)	380	2.54	2.60	2.08	2.02
Diethyl Disulfide	300	2.79	2.86	2.26	2.19
($C_4H_{10}S_2$)	380	2.74	2.81	2.22	2.15
Methyl Thioacetate	300	2.11	2.16	1.75	1.70
(C_3H_6OS)	380	2.09	2.13	1.73	1.68
3-Mercaptohexan-1-ol	300	2.55	2.62	2.08	2.02
($C_6H_{14}OS$)	380	2.52	2.59	2.06	2.00
4-Mercapto-4-	300	2.86	2.95	2.31	2.24
methylpentan-2-one	380	2.80	2.88	2.27	2.20
($C_6H_{12}OS$)					
4-Mercapto-4-	300	3.08	3.16	2.45	2.39
methylpentan-2-ol	380	3.00	3.08	2.40	2.34
($C_6H_{14}OS$)					
Benzothiazole	300	2.46	2.51	2.01	1.95
(C_7H_5NS)	380	2.44	2.50	2.00	1.94
2-Furanmethanethiol	300	2.59	2.65	2.09	2.04
(C_5H_6OS)	380	2.54	2.61	2.06	2.01
2-Mercaptoethanol	300	2.97	3.04	2.45	2.40
(C_2H_6OS)	380	2.85	2.92	2.36	2.30
Benzenemethanethiol	300	2.51	2.57	2.05	1.99
(C_7H_8S)	380	2.49	2.55	2.04	1.98
2-Mercaptoethyl	300	2.46	2.51	1.99	1.93
acetate	380	2.42	2.47	1.96	1.90
($C_4H_8O_2S$)					
3-mercaptopropyl	300	2.44	2.50	1.98	1.92
acetate	380	2.42	2.47	1.96	1.90
($C_5H_{10}O_2S$)					
Cis-3,6-dimethyl-	300	2.50	2.56	2.04	1.99
1,2,4,5-tetrathiane	380	2.50	2.56	2.04	1.99
($C_4H_8S_4$)					
Prenyl-mercaptan	300	2.55	2.61	2.08	2.03
($C_5H_{10}S$)	380	2.51	2.57	2.02	2.01
Trans-3,6-dimethyl-	300	2.45	2.52	2.01	1.95
1,2,4,5-tetrathiane	380	2.45	2.52	2.01	1.95
($C_4H_8S_4$)					
2-Methyl-3-furanthiol	300	2.12	2.18	1.75	1.71
(C_5H_6OS)	380	2.12	2.17	1.75	1.70
2-Methylthiolane-3-ol	300	2.69	2.76	2.17	2.12
($C_5H_{10}OS$)	380	2.63	2.70	2.13	2.08
3-Mercapto-3-	300	2.55	2.62	2.07	2.02
methylbutan-1-ol	380	2.52	2.58	2.04	1.99
($C_5H_{12}OS$)					
Ethyl-3-	300	3.23	3.32	2.57	2.49
mercaptopropionate	380	3.13	3.21	2.50	2.42
($C_5H_{10}O_2S$)					
5-2-hydroxyethyl-	300	3.27	3.37	2.60	2.51
4-methylthiazole	380	3.17	3.27	2.53	2.45
(C_6H_9NOS)					
2-Methyltetrahydro	300	2.41	2.47	1.96	1.91
thiophen-3-one	380	2.37	2.44	1.93	1.88
(C_5H_8OS)					
3-Methylsulfanyl	300	3.50	3.59	2.84	2.76
propan-1-ol	380	3.36	3.45	2.73	2.65
($C_4H_{10}OS$)					
3-	300	2.66	2.73	2.15	2.10
Mercaptohexylacatate	380	2.64	2.72	2.14	2.09
($C_8H_{16}O_2S$)					
Ethylthioacetate	300	2.24	2.29	1.84	1.79
(C_4H_8OS)	380	2.22	2.27	1.82	1.77

would be affected only marginally, with the result that the quantification of the VOSCs by this method remains reliable.

5. Concluding remarks

We evaluate and report CI-MS rate coefficients for ion-molecule reactions associated with a number of reagent ions (H_3O^+, NH_4^+, NO^+, and O_2^+) to a comprehensive list of VOSCs related to spoiled food and beverages. The electric dipole moment and polarizability of the neutral VOSCs are the input ingredients for the rate-coefficient calculations. We compute these parameters by DFT simulations. The computed parameters are in good agreement with the available experimental/theoretical values. We additionally provide molecular properties such as the PA and IE, useful in the determination of the exothermal nature of a given reaction, and correspondingly for the selection of appropriate reagent ions in CI-MS techniques. For example, one could decide that ionization via NH_4^+-CI-MS is advantageous for the quantification of such species where ionization with H_3O^+ produces multiple fragments. We evaluate these rate coefficients applying state-of-the-art capture collision model, frequently used for highly energetic PTR-MS conditions, using parametrized trajectory method at commonly exploited experimental conditions. Generally, rates obtained by parametrized trajectory method at center-of-mass energy are best suited for the high effective temperature of PTR-MS drift tube.

The PTR/SRI-MS reaction kinetics data reported in the present work make available a useful resource for determining the concentrations of VOSCs. They can thus find a broad application in the quality assessment of several food products.

Author contributions

M.B. made all simulations and arranged the data tables. N.M. supervised the theoretical modeling, F.B. and L.C. suggested the problem and the compounds worth investigating. All authors contributed to writing the manuscript.

Declaration of competing interest

The authors declare that they have no known competing financial interests or personal relationships that could have appeared to influence the work reported in this paper.

Acknowledgements

The authors are grateful to CINECA for providing computational resources through the Iscra C “k-ADO” project. Financial support from Fondazione Edmund Mach (ADP, 2018) is also highly appreciated.

Appendix A. Supplementary data

Supplementary data to this article can be found online at https://doi.org/10.1016/j.ijms.2022.116860.

References

[1] K. Ridgway, S. Lalljie, R. Smith, Analysis of food taints and off-avours - a review, Food Addit. Contam. 27 (2010) 146–168.
[2] M. Qian, X. Fan, K. Mahattanatawee, In Volatile Sulfur Compounds in Food; ACS Symposium Series, Oxford University Press USA, 2012.
[3] M.E. Smith, M. Bekker, P. Smith, E. Wilkes, Sources of volatile sulfur compounds in wine, Aust. J. Grape Wine Res. 21 (2015) 705–712.
[4] In Understanding Wine Chemistry (Chapter 10), John Wiley & Sons, Ltd, 2016, pp. 88–98.
[5] J. Goode, Mercaptans and Other Volatile Sulfur Compounds in Wine, Harpers Wine & Spirit Weekly, 2006.
[6] D. Fracassetti, In Occurrence and Analysis of Sulfur Compounds in Wine, IntechOpen, 2018.
[7] A. Hansel, A. Jordan, R. Holzinger, P. Prazeller, W. Vogel, W. Lindinger, Proton transfer reaction mass spectrometry: on-line trace gas analysis at the ppb level, Int. J. Mass Spectrom. Ion Process. 149–150 (1995) 609–619.
[8] P. Španěl, D. Smith, Selected ion ow tube: a technique for quantitative trace gas analysis of air and breath, Med. Biol. Eng. Comput. 34 (1996) 409–419.
[9] G. Eerdekens, L.N. Ganzeveld, J. Vilà -Guerau de Arellano, T. Klüpfel, V. Sinha, Flux estimates of isoprene, methanol and acetone from airborne PTR-MS measurements over the tropical rainforest during the GABRIEL 2005 campaign, Atmos. Chem. Phys. 9 (2009) 4207–4227.
[10] J.D. Pleil, A. Hansel, J. Beauchamp, Advances in proton transfer reaction mass spectrometry (PTR-MS): applications in exhaled breath analysis, food science, and atmospheric chemistry, J. Breath Res. 13 (2019) 039002.
[11] M.-Á. Pozo-Bayón, J.-P. Schirlè -Keller, G.A. Reineccius, Determining specific food volatiles contributing to PTR-MS ion profiles using GC-EI-MS, J. Agric. Food Chem. 56 (2008) 5278–5284.
[12] I.A. Hanouneh, N.N. Zein, F. Cikach, L. Dababneh, D. Grove, N. Alkhouri, R. Lopez, R.A. Dweik, The breath-prints in patients with liver disease identify novel breath bio-markers in alcoholic hepatitis, Clin. Gastroenterol. Hepatol. 12 (2014) 516–523.
[13] E. Schuhfried, M. Probst, J. Limtrakul, S. Wannakao, E. Aprea, L. Cappellin, T. Märk, F. Gasperi, F. Biasioli, Sulfides: chemical ionization induced fragmentation studied with Proton Transfer Reaction-Mass Spectrometry and density functional calculations, J. Mass Spectrom. 48 (2013) 367–378.
[14] W. Harper, N. Kocaoglu-Vurma, C. Wick, K. Elekes, V. Langford, Analysis of volatile sulfur compounds in Swiss cheese using selected ion flow tube mass spectrometry (SIFT-MS), ACS (Am. Chem. Soc.) Symp. Ser. 1068 (2011) 153–181.
[15] V. Perraud, S. Meinardi, D. Blake, B. Finlayson-Pitts, Challenges associated with the sampling and analysis of organosulfur compounds in air using real-time PTR-ToF-MS and off-line GC-FID, Atmos. Meas. Tech. Discuss. 8 (2015) 13157–13197.
[16] L. Cappellin, M. Probst, J. Limtrakul, F. Biasioli, E. Schuhfried, C. Soukoulis, T.D. Märk, F. Gasperi, Proton transfer reaction rate coefficients between H_3O^+ and some sulphur compounds, Int. J. Mass Spectrom. 295 (2010) 43–48.
[17] A.M. Ellis, C.A. Mayhew, In Proton Transfer Reaction Mass Spec- Trometry Principles and Applications, John Wiley & Sons, Chichester, United Kingdom, 2014.
[18] T. Su, M.T. Bowers, Theory of ion-polar molecule collisions. Comparison with experimental charge transfer reactions of rare gas ions to geometric isomers of diuorobenzene and dichloroethylene, J. Chem. Phys. 58 (1973) 3027–3037.
[19] T. Su, M. T. Bowers, Ion-Polar molecule collisions: the effect of ion size on ion-polar molecule rate constants; the parameterization of the average-dipole-orientation theory, Int. J. Mass Spectrom. Ion Phys. 12 (1973) 347–356.
[20] T. Su, W.J. Chesnavich, Parametrization of the ion-polar molecule collision rate constant by trajectory calculations, J. Chem. Phys. 76 (1982) 5183–5185.
[21] T. Su, Parametrization of kinetic energy dependence of ion–polar molecule collision rate constants by trajectory calculations, J. Chem. Phys. 100 (1994) 4703.
[22] P. Španěl, D. Smith, Selected ion ow tube studies of the reactions of H_3O^+, NO^+ and O_2^+ with some organosulphur molecules, Int. J. Mass Spectrom. 176 (1998) 167–176.
[23] L. Cappellin, T. Karl, M. Probst, O. Ismailova, P.M. Winkler, C. Soukoulis, E. Aprea, T.D. Märk, F. Gasperi, F. Biasioli, On quantitative determination of volatile organic compound concentrations using proton transfer reaction time-of-flight mass spectrometry, Environ. Sci. Technol. 46 (2012) 2283–2290.
[24] A. Midey Jr, S. Williams, T. Miller, A. Viggiano, Reactions of O_2^+ , NO^+ and H_3O^+ with methylcyclohexane (C_7H_{14}) and cyclooctane (C_8H_{16}) from 298 to 700 K, Int. J. Mass Spectrom. 222 (2003) 413–430.
[25] A. Jordan, S. Haidacher, G. Hanel, E. Hartungen, J. Herbig, L. Märk, R. Schottkowsky, H. Seehauser, P. Sulzer, T. Märk, An online ultra-high sensitivity Proton-transfer-reaction mass-spectrometer combined with switchable reagent ion capability PTR+SRI-MS, Int. J. Mass Spectrom. 286 (2009) 32–38.
[26] P. Sulzer, A. Edtbauer, E. Hartungen, S. Jürschik, A. Jordan, G. Hanel, S. Feil, S. Jaksch, L. Märk, T.D. Märk, From Conventional Proton-Transfer-Reaction Mass Spectrometry, PTR-, 2012.
[27] M. Lanza, W. Acton, K. Breiev, S. Jürschik, R. Gutmann, A. Jordan, E. Hartungen, G. Hanel, J. Herbig, L. Märk, C. Mayhew, T. Märk, P. Sulzer, In Selected-Reaget-Ionization Mass Spectrometry (SRI-MS): Advancements in Instrumentation and Novel Applications, 2015.
[28] G.H. Wannier, On the motion of gaseous ions in a strong electric field, I. Phys. Rev. 83 (1951) 281–289.
[29] G.H. Wannier, Motion of gaseous ions in strong electric fields, Bell Syst. Tech. J. 32 (1953) 170–254.
[30] M. McFarland, D.L. Albritton, F.C. Fehsenfeld, E.E. Ferguson, A.L. Schmeltekopf, Flow-drift technique for ion mobility and ionmolecule reaction rate constant measurements. II. Positive ion reactions of N^+, O^+, and H_2^+ with O_2 and O^+ with N_2 from thermal to ~ 2 eV, J. Chem. Phys. 59 (1973) 6620–6628.
[31] K. Buhr, S. van Ruth, C. Delahunty, Analysis of volatile avour compounds by Proton Transfer Reaction-Mass Spectrometry: fragmentation patterns and discrimination between isobaric and isomeric compounds, Int. J. Mass Spectrom. 221 (2002) 1–7.
[32] K.P. Wyche, R.S. Blake, K.A. Willis, P.S. Monks, A.M. Ellis, Differentiation of isobaric compounds using chemical ionization reaction mass spectrometry, Rapid Commun. Mass Spectrom. 19 (2005) 3356–3362.
[33] E. Canaval, N. Hyttinen, B. Schmidbauer, L. Fischer, A. Hansel, NH_4^+ association and proton transfer reactions with a series of organic molecules, Front. Chem. 7 (2019).
[34] L. Cappellin, S. Makhoul, E. Schuhfried, A. Romano, J. Sanchez del Pulgar, E. Aprea, B. Farneti, F. Costa, F. Gasperi, F. Biasioli, Ethylene: absolute real-time high-sensitivity detection with PTR/SRI-MS. The example of fruits, leaves and bacteria, Int. J. Mass Spectrom. 365–366 (2014) 33–41.
[35] A.R. Koss, C. Warneke, B. Yuan, M.M. Coggon, P.R. Veres, J.A. de Gouw, Evaluation of NO^+ reagent ion chemistry for online measurements of atmospheric volatile organic compounds, Atmos. Meas. Tech. 9 (2016) 2909–2925.
[36] M.J. Frisch, G.W. Trucks, H.B. Schlegel, G.E. Scuseria, M.A. Robb, J.R. Cheeseman, G. Scalmani, V. Barone, G.A. Petersson, H. Nakatsuji, X. Li, M. Caricato, A.V. Marenich, J. Bloino, B.G. Janesko, R. Gomperts, B. Mennucci, H.P. Hratchian, J.V. Ortiz, A.F. Izmaylov, J.L. Sonnenberg, D. Williams-Young, F. Ding, F. Lipparini, F. Egidi, J. Goings, B. Peng, A. Petrone, T. Henderson, D. Ranasinghe, V.G. Zakrzewski, J. Gao, N. Rega, G. Zheng, W. Liang, M. Hada, M. Ehara, K. Toyota, R. Fukuda, J. Hasegawa, M. Ishida, T. Nakajima, Y. Honda, O. Kitao, H. Nakai, T. Vreven, K. Throssell, J.A. Montgomery Jr, J.E. Peralta, F. Ogliaro, M.J. Bearpark, J.J. Heyd, E.N. Brothers, K.N. Kudin, V.N. Staroverov, T.A. Keith, R. Kobayashi, J. Normand, K. Raghavachari, A.P. Rendell, J.C. Burant, S.S. Iyengar, J. Tomasi, M. Cossi, J.M. Millam, M. Klene, C. Adamo, R. Cammi, J.W. Ochterski, R.L. Martin, K. Morokuma, O. Farkas, J.B. Foresman, D.J. Fox, Gaussian 16 Revision C.01, Gaussian Inc., Wallingford CT, 2016.
[37] C. Lee, W. Yang, R.G. Parr, Development of the Colle-Salvetti correlation-energy formula into a functional of the electron density, Phys. Rev. B 37 (1988) 211–212.
[38] NIST data-base., https://webbook.nist.gov/chemistry/, Accessed: 30- 08-2020.
[39] PubChem data-base., https://pubchem.ncbi.nlm.nih.gov/, Accessed: 30-08-2020.
[40] R. Li, C. Warneke, M. Graus, R. Field, F. Geiger, P.R. Veres, J. Soltis, S.-M. Li, S.M. Murphy, C. Sweeney, G. Pètron, J.M. Roberts, J. de Gouw, Measurements of hydrogen sulfide (H_2S) using PTRMS: calibration, humidity dependence, inter-comparison and results from field studies in an oil and gas production region, Atmos. Meas. Tech. 7 (2014) 3597–3610.
[41] T. Fujii, In Ion-Molecule Attachment Reactions: Mass Spectrometry, Springer US, 2015.
[42] G.J. Francis, P.F. Wilson, D.B. Milligan, V.S. Langford, M.J. McEwan, GeoVOC: a SIFT-MS method for the analysis of small linear hydrocarbons of relevance to oil exploration, Int. J. Mass Spectrom. 268 (2007) 38–46.
[43] P. Španěl, T. Wang, D. Smith, A selected ion ow tube, SIFT, study of the reactions of H_3O^+, NO^+ and O_2^+ ions with a series of diols, Int. J. Mass Spectrom. 218 (2002) 227–236.
[44] P. Spanel, T.S. Wang, D. Smith, A selected ion ow tube, SIFT, study of the reactions of H_3O^+, NO^+ and O_2^+ ions with a series of diols, Int. J. Mass Spectrom. 218 (2002) 227–236.
[45] Harrison, A. G., In, Harrison, A. G., Ed.; Taylor & Francis: 1992, pp 71–90.
[46] W.M. Haynes, In CRC Handbook of Chemistry and Physics, 100 Key Points, 96th Edition, CRC Press, 2015.
[47] C.L. Yaws, In Thermophysical Properties of Chemicals and Hydrocarbons, Elsevier Science, 2008.
[48] J. Zhao, R. Zhang, Proton transfer reaction rate constants between hydronium ion (H_3O^+) and volatile organic compounds (VOCs), Atmos. Environ. 38 (2004) 2177–2185.